
This is the **accepted version** of the journal article:

Vélez, Paris; Martín, Ferran; Fernández-García, Raúl; [et al.]. «Embroidered textile frequency-splitting sensor based on stepped-impedance resonators». IEEE sensors journal, Vol. 22, Issue 9 (May 2022), p. 8596-8603. DOI 10.1109/JSEN.2022.3163165

This version is available at <https://ddd.uab.cat/record/258463>

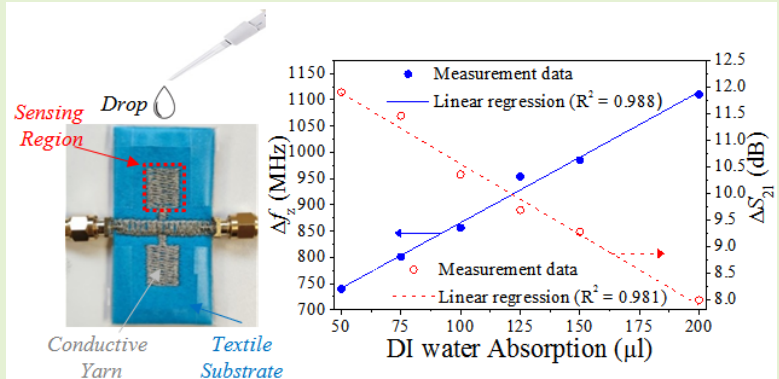
under the terms of the  ^{IN} COPYRIGHT license

Embroidered Textile Frequency-Splitting Sensor based on Stepped-Impedance Resonators

Paris Vélez, *Senior Member, IEEE*, Ferran Martín, *Fellow, IEEE*, Raúl Fernández-García, and Ignacio Gil

Abstract— This paper presents an embroidered textile frequency-splitting microwave sensor based on a pair of identical stepped-impedance resonators (SIRs) loading a microstrip transmission line. The sensor is implemented by means of conductive threads. The sensing region of the proposed structure is the capacitive square patch of one of the SIRs. If such region is kept unaltered, the structure is symmetric, and the frequency response (transmission coefficient) exhibits a single transmission zero. However, if symmetry is broken (e.g., through liquid absorption in the sensing region), the frequency response of the proposed sensor exhibits two transmission zeros (frequency splitting). The difference (in frequency and magnitude) between such zeros (or notches) is intimately related to the dielectric properties of the absorbed liquids to be sensed/detected. The proposed sensing structure is applied to the detection of deionized (DI) water absorption, and to the quantification of the number of DI water drops. The maximum measured sensitivity is found to be 2.70 MHz/ μl and 0.03 dB/ μl for the incremental frequency and incremental magnitude of the notches.

Index Terms— Absorption, conductive yarn, dielectric constant, drops, embroidered sensor, frequency splitting, microstrip, microwave sensors.



I. INTRODUCTION

WEARABLE electronics and electronic textiles (e-textiles) areas are attracting the attention of researchers in the last years. One of the most important aspects that offer these two technological areas resides in the possibility to integrate the electronic components and complete systems directly into the textile substrate. This fact has allowed the printing of passive electronic components [1-3] and embroidering directly on textile substrates by means of conductive threads [4-6]. This fact has opened a new door in the design of microwave circuits, more specifically in the design of wearable textile RF/microwave components (e.g. filters and antennas) and sensors [7-14]. Today, wearable e-textile technologies are experiencing a massive growth due to

the properties they provide, especially in the field of sensors, such as wash ability, and full direct implementation on the clothes [15-16]. On the other hand, planar microwave sensors can potentially satisfy many demanding requirements and provide technical solutions to several challenging aspects due to their low cost, small size and low profile. Also, microwave planar sensors can be implemented in many different types of substrates, including flexible and textile substrates.

In the recent literature, various strategies have been proposed for the optimization of the sensitivity (one of the most important performance parameters in sensors) in planar microwave sensors implemented on rigid substrates. Most of these works are based on the use of non-resonant [17, 18] and resonant [19-22] structures. In the latter case, the most extended working principle exploits the resonance frequency variation due to the dielectric properties of the materials (solids and liquids) under test (MUT). However, there are also resonant sensors where frequency splitting is the sensing mechanism [23]. Planar microwave sensors, either non-resonant or resonant, can be implemented by considering reflective-mode [24, 25] or transmission-mode [18, 22, 23] structures, and using single-ended [19-22] or differential measurement techniques [26-28]. Many reported sensors to date exhibit very good performance (high sensitivity, high resolution, low cost and easy fabrication process), and have

This work was supported by MICIIN-Spain (projects PID2019-103904RB-I00, TEC2016-79465-R, and PDC2021-121085-I00), Generalitat de Catalunya (project 2017SGR-1159), Institució Catalana de Recerca i Estudis Avançats (who awarded Ferran Martín), and by FEDER funds.

P. Vélez, and F. Martín are with GEMMA/CIMITEC, Departament d'Enginyeria Electrònica, Universitat Autònoma de Barcelona, 08193, Bellaterra, Spain (email: paris.velez@uab.cat).

R. Fernández-García, and I. Gil are with Departament of Electronic Engineering, Universitat Politècnica de Catalunya (UPC), Terrassa, Spain.

been applied to the dielectric characterization of solids [18], liquids [23], liquid composition detection [29], or defect detection in samples [27], among others.

Frequency-splitting sensors (the subject of interest in this paper) can be implemented following several strategies, but the simplest one utilizes two identical sensing resonant elements, symmetrically loading a host transmission line. Sensing is based on the splitting in the resonance frequency that result by symmetry perturbation. The most usual procedure for symmetry truncation in pairs of resonant elements is by placing asymmetric dielectric loads on top of such resonators. Consequently, most reported frequency-splitting sensors have been applied to the dielectric characterization of solids and liquids. Such sensors are able to detect differences between the so-called reference (REF) sample, placed on top of one of the resonant elements of the pair, and the sample (or material) under test (MUT), situated on top of the other resonator.

This paper demonstrates, for the first time, the symmetry properties of frequency-splitting microwave sensors implemented in textile substrates. The proposed topology is based on the work presented in [30], where frequency-splitting sensors based on stepped impedance resonators (SIRs) [31] and implemented in rigid substrates were proposed. The frequency of operation of the textile sensor presented in this paper is set to 3 GHz, and the sensor is applied to the characterization of liquid absorption and drop detection. High sensitivities and good repetitively in the measurements of different prototypes are obtained, as it will be shown.

The paper is organized as follows. Section II presents the sensor topology (including the equivalent circuit model), the layout design of the proposed sensor, and the principle of operation, considering the electric properties of textile commercial materials (substrate and conductive threads [32, 33]). In Section III, the fabrication process of the presented textile microwave sensor is detailed and validated through simulation and measurement of the bare sensor. The results derived from this work concerning the characterization of the amount of deionized (DI) water absorbed by the textile substrate of the sensor, as well as the detection of drops of small volume, are presented in Section IV. A comparison with other textile microwave sensors for absorption characterization is carried out in Section V. Finally, Section VI summarizes the relevant conclusions of the presented work.

II. SENSOR TOPOLOGY AND PRINCIPLE OF OPERATION

The proposed frequency-splitting sensing structure, first reported in [30], is based on a microstrip transmission line loaded with a pair of mirrored stepped-impedance resonators (SIRs) magnetically coupled (such magnetic coupling is consequence of the proximity between the narrow inductive strips of the SIRs). The layout and the equivalent circuit model (including dielectric losses) are shown in Fig. 1. The host microstrip line is described by the transmission line sections at both sides of the SIRs, with characteristic impedance Z_0 and electrical length kl , where k and l are the phase constant and

physical length, respectively. In reference to the SIRs, the narrow strip and the rectangular patch are modeled by the inductance L_{si} and capacitance C_{si} , respectively, where $i = 1, 2$ denote the specific SIR. The dielectric losses are taken into account by means of the resistance R_{ci} , parallel connected to the SIR capacitance, and the magnetic coupling between resonators is described by the mutual inductance M (with negative sign due to the opposite directions of the current lines through the SIRs [see Fig.1(b)]).

Note that the equivalent circuit model is not symmetric. The reason is the disruption of symmetry caused by the presence of a dielectric load (with complex permittivity $\epsilon^* = \epsilon' - j\epsilon''$) in the sensing region. The sensing region is the textile substrate zone corresponding to the capacitive patch of the SIR designated as 1 in Fig. 1. Thus, varying C_{s1} and R_{c1} can model any change in the complex dielectric constant (real and imaginary parts respectively) of the solid/liquid under test. If the structure is symmetric, corresponding to an absence of dielectric load in the sensing region, then $L_{s1} = L_{s2}$; $C_{s1} = C_{s2}$; $R_{c1} = R_{c2}$, and the transmission coefficient exhibits a single transmission zero at the resonance frequency given by [30]

$$\omega_0 = 2\pi f_0 = \frac{1}{\sqrt{(L_{s1,2} - |M|)C_{s1,2}}} \quad (1)$$

By contrast, if symmetry is disrupted (caused by a dielectric material in contact with the sensing region or by changes in the substrate in that region), a split in frequency appears, causing the appearance of an additional resonance. Considering $L_{s1} = L_{s2} = L_s$ (the inductances are not affected by the presence of absorbed liquid in the considered volume range), the two resonance (angular) frequencies are given by

$$\omega_{\pm} = \sqrt{\frac{L_s(C_{s1} + C_{s2}) \pm \sqrt{[L_s(C_{s1} - C_{s2})]^2 + 4C_{s1}C_{s2}M^2}}{2C_{s1}C_{s2}(L_s^2 - M^2)}} \quad (2)$$

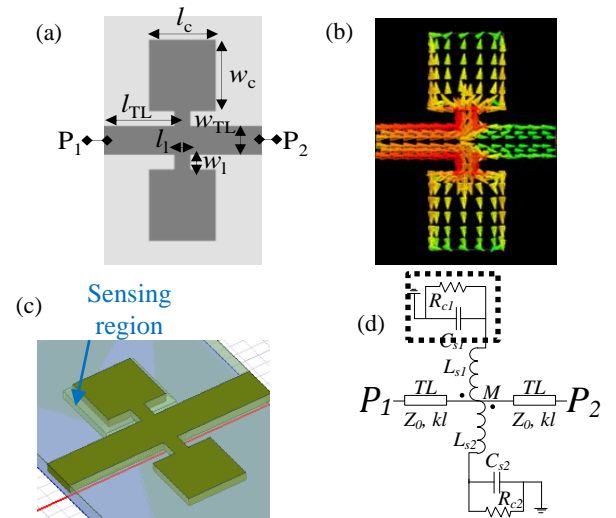


Fig.1. 2D Layout (a), electric field distribution at the resonance frequency (f_0) of the coupled SIRs (b), 3D HFSS layout view (c), and equivalent circuit model (d) of the proposed differential microwave sensor. The ground plane is depicted in soft grey color. The relevant dimensions are indicated.

In Fig. 2, the resonance frequencies are designated as f_1 and f_2 , and are related to the angular resonances of expression (2) by $f_1 = \omega/2\pi$ and $f_2 = \omega/2\pi$. In such figure, circuit responses corresponding to the symmetric case and two asymmetric cases are depicted. Note that for the asymmetric responses, only the capacitor C_{s1} changes (the other electrical parameters are kept unaltered).

To illustrate the electromagnetic behavior of the proposed differential sensor, let us consider the topology shown in Fig. 1(c). Fig. 3 shows the full 3D electromagnetic simulation (using the *Ansys HFSS* simulator) of the transmission coefficient of the layout of Fig. 1(c), considering different substrate dielectric conditions. The sensitive region (see Fig. 1c) has been defined with a hypothetical material that emulates the textile substrate conditions when liquid absorption occurs. It is assumed that the liquid does not reach the line region (a reasonable hypothesis for moderate absorption in the sensitive region). The real and the imaginary part of the complex dielectric constant (ϵ' , ϵ'') of this material has been linearly increased from the initial value of the textile substrate, i.e., $\epsilon' = 1.30$ and $\epsilon'' = 0.00585$, up to $\epsilon' = 2.75$ and $\epsilon'' = 0.0123$. As it can be expected, when the dielectric constant of the sensitive region coincides with the nominal one (symmetric configuration), the transmission coefficient exhibits only a single notch in the vicinity 3 GHz. If the symmetry is truncated by changes in the conditions of the substrate in one of the SIR with respect to the other, frequency splitting arises (Fig. 3). Under these conditions, the difference in frequency (Δf_z) and magnitude (ΔS_{21}) between the two generated transmission zeros can be related to the differential complex dielectric constant of the MUT, with real and imaginary parts designated by $\Delta\epsilon'$ and $\Delta\epsilon''$.

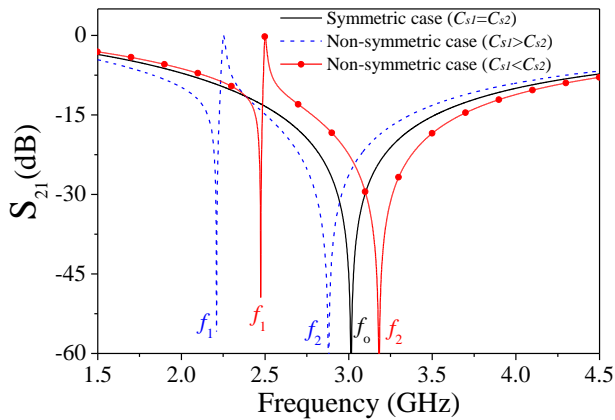


Fig.2. Typical frequency response of the transmission coefficient (excluding losses and the transmission lines sections) of the equivalent circuit of Fig. 1(d). The considered circuit parameters are: $L_{s1,2} = 2.00$ nH, $C_{s2} = 1.85$ pF, $M = -0.49$, and $C_{s1} = 1.85$ pF, $C_{s1} = 2.30$ pF and $C_{s1} = 1.50$ pF for the three considered cases.

Due to the quasi-linear dependence of the complex dielectric constant with Δf_z and ΔS_{21} (see Fig. 4), the changes in both the real and the imaginary parts of the complex dielectric constant can be expressed as [34, 35]:

$$\Delta\epsilon' = k_{11}\Delta f_z + k_{12}\Delta S_{21} \quad (3a)$$

$$\Delta\epsilon'' = k_{21}\Delta f_z + k_{22}\Delta S_{21} \quad (3b)$$

where k_{ij} (with $j = 1,2$ and $i = 1,2$) are coefficients that can be deduced from the simulated data points of Fig. 4.

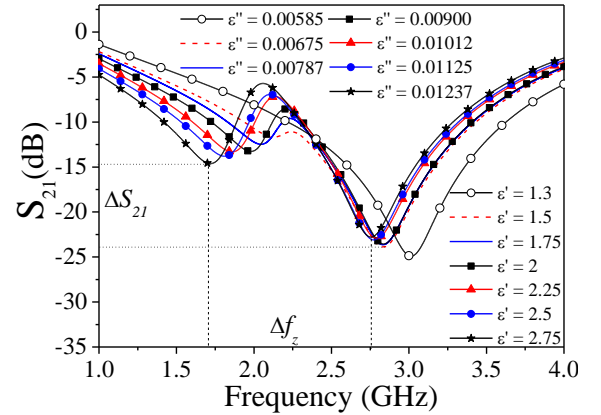


Fig.3. Simulated frequency response of the transmission coefficient of the sensor of Fig. 1(c) considering different complex dielectric constants. The geometrical parameters in reference to Fig. 1(a) are: $w_{TL} = 5.89$ mm, $l_{TL} = 15$ mm, $l_c = 12.5$ mm, $w_c = 14.5$ mm, $l_l = 3$ mm, $w_l = 3$ mm.

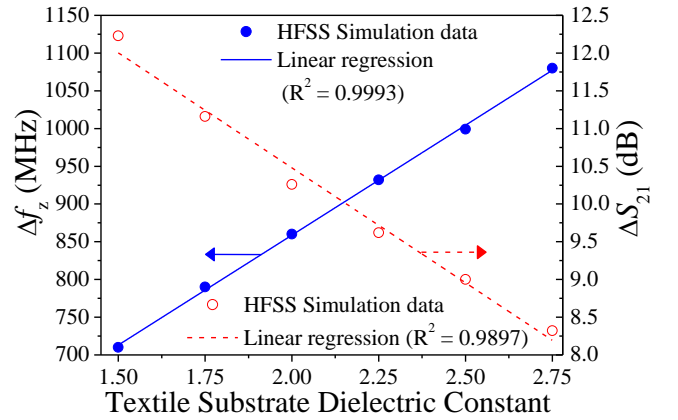


Fig.4. Representation of simulated $\Delta f_z = f_2 - f_1$ and $\Delta S_{21} = S_{21min,f2} - S_{21min,f1}$ as a function of the dielectric properties of the considered textile substrate for the implementation of real differential sensor. Note that the horizontal axis corresponds to the real part of the complex dielectric constant of the MUT. The corresponding values of the imaginary part can be deduced from the insets of Fig. 3.

The following section describes the sensor fabrication process to implement the textile frequency-splitting microwave sensor prototype and the validation of the proper definition of the different materials in the 3D simulator software. The equivalent circuit model of Fig. 2(d) is also validated.

III. SENSOR FABRICATION AND VALIDATION

To obtain a textile frequency-splitting microwave sensor operating at $f_0 = 3$ GHz, a two layer of non-woven 100% polyester (PES) textile material (each one of 0.80 mm thickness) with permittivity $\epsilon_r = 1.30$ is considered. The dielectric loss tangent is $\tan \delta = 0.0045$. The considered textile substrate has advantages, such as a high resistance to breakage by penetration and lightweight (weight of 211 g/m²). One layer of textile substrate has been covered with an adhesive

copper of 35 μm thickness and conductivity $5.8 \cdot 10^7$ S/m to act as the ground plane of the structure. The embroidered metallic conductor (that includes the 50- Ω host microstrip transmission line and the SIRs) in layer 2 has implemented by means of a *Singer Futura XL550* sewing machine, considering conductive thread (commercial *Shieldex 117/17* 2-ply with 99% pure silver-plated nylon yarn 140/17 *dtex*) [36]. The embroidery technique for the sensor has been done by means of a satin fill pattern creating rows of stitches. Regarding the embroidery setup, a weave fill pattern with stitch spacing (distance between two consecutive stitches) and stitch length of 0.45 mm and 5 mm, respectively, has been considered (the linear resistance is less than 30 Ω /cm [36]).

After soldering the 50- Ω 3.5-mm connectors to the ground plane, the signal path has been fixed interlacing it with the conductive fibers of the yarn. A photograph of the fabricated sensor prototype is depicted in Fig. 5. Note that the two textile dielectric layers have been glued with a specific spray and finally sealed with insulating tape in order to avoid air gap effects. With the considered substrate parameters, the width of the microstrip line provides a characteristic impedance of $Z_0 = 50 \Omega$ (matched to the reference impedance of the ports).

The measured transmission coefficient (magnitude and phase) of the prototype of Fig. 5 is plotted in Fig. 6. The frequency response inferred by the layout of Fig. 1(c) (considering the geometrical parameters of the figure caption in Fig. 3), and the response of the circuit of Fig. 1(d), are included in order to validate the proper definition of the different materials in the 3D Simulator. The electrical parameter extraction has been done by considering a single SIR loading a microstrip line, and using the scattering parameters [37] obtained from the *HFSS* electromagnetic simulator. Finally, the inductive coupling coefficient M has been obtained by curve fitting. The agreement between the three curves is good in the considered frequency range. The measured frequency and magnitude of the transmission zero is 3.09 GHz (2.2% of variation respect to the simulated one) and -24.937 dB (0.1% of variation respect to the simulated one). It should be noted that a high level of symmetry has been obtained (essential for the correct operation of the sensor/comparator), since the fabricated prototype exhibits only one transmission zero.

Once the prototype has been fabricated, the next step is to validate the electromagnetic sensor performance through absorption of DI water, that produces a variation in the complex dielectric constant (ϵ^*) of the textile substrate in the sensitive region (the area below the capacitive patch of SIR).

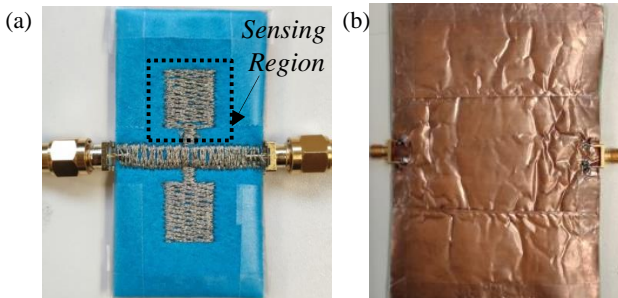


Fig. 5. Top (a) and bottom (b) views of the fabricated textile microwave frequency-splitting sensor. The sensing region is indicated.

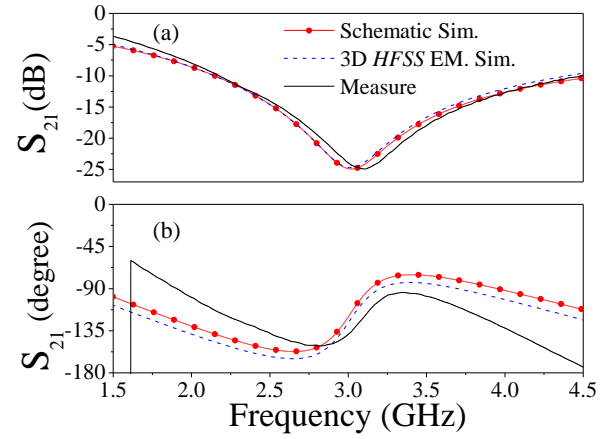


Fig. 6. Transmission coefficient magnitude (a) and phase (b) corresponding to the sensor of Fig. 5 (symmetric case). The electrical parameters in reference to the equivalent circuit model of Fig. 1(d) are: $L_{s1,2} = 2.00$ nH, $C_{s1,2} = 1.85$ pF, $R_{c1,2} = 184 \Omega$, $Z_0 = 50 \Omega$, $kl = 61^\circ$ and $M = -0.49$.

IV. EXPERIMENTAL RESULTS

To experimentally validating the proposed microwave frequency-splitting sensor, i.e., its capability to detect permittivity-related changes in the sensing region, absorption tests have been carried out. Note that this is the interest of this work, rather than determining the complex dielectric constant of a certain liquid under test (for that purpose, sensors based on low-loss microwave substrates are preferred). The considered liquid to be absorbed is DI water, with a complex dielectric constant of $\epsilon^* = 78.11 - j12.81$ at 3 GHz. Both the real and the imaginary parts of the complex dielectric constant of DI water are significantly higher than those of the considered textile substrate (with $\epsilon' = 1.30$ and $\epsilon'' = 0.00585$). Therefore, the effective dielectric constant of the sensing zone should increase when DI water is absorbed. Because of that, frequency splitting is expected, and two resonances should appear. Indeed, the two resonances, or notches, should be situated to the left of f_0 , the resonance frequency for the symmetric case (where absorption is absent). The different transmission coefficients (obtained by means of a handheld 2-port *Keysight N9923A Fieldfox RF vector network analyzer*) of the sensor of Fig. 5, considering absorption of DI water in the volume range between 50 μl and 200 μl , are shown in Fig. 7. The different measurements have been made with a precision pipette with an operating range between 1 μl – 1000 μl .

As expected, frequency splitting increases with the amount of absorbed liquid. The difference between the notch frequency position ($\Delta f_z = f_2 - f_1$) and notch magnitude ($\Delta S_{21} = S_{21min,f2} - S_{21min,f1}$) increases and decreases, respectively, as the amount of absorbed DI water increases, in coherence with the results of Fig. 4. The measured (average) sensitivity is 2.56 MHz/ μl and 0.027 dB/ μl for the differential frequency and differential notch depth, the output variables. Due to the reasonable good linearity (see Fig. 8) of the sensor response (for both Δf_z and ΔS_{21}), the amount of absorbed DI water in the sensitive region (the square patch capacitor indicated in Fig. 5) can be calculated as follows

$$\text{Absorption } (\mu\text{l}) = -244.59 + 0.39(\Delta f_z) \quad (4a)$$

$$\text{Absorption } (\mu\text{l}) = 490.90 - 37.02(\Delta S_{21}) \quad (4b)$$

with a square correlation coefficient of $R^2 = 0.986$ and $R^2 = 0.981$ respectively.

To ensure that the sensor does not experience any potential memory effect between the different measurements, the sensing region has been dried after each measurement. For that purpose, an air dryer has been used. The measured curves are plotted in Fig. 9, where it can be seen that such curves are roughly undistinguishable and exhibit a single transmission zero at f_0 , indicative of sensor symmetry. Nevertheless, the measured curves (indicative of the recovery state for the frequency-splitting sensor) exhibit a variability in frequency and magnitude of 1.8% and 4.1% respectively, at f_0 , i.e., perfectly acceptable.

In order to evaluate the repeatability of the measurements, two additional textile frequency-splitting microwave sensors (A and B) have been fabricated using an identical process to that of the sensor of Fig. 5 (see Fig. 10). For these new sensors, the same measurements carried out with the sensor of Fig. 5 have been performed. However, in sensor A, the different measurements have been done by gradually increasing the amount of DI water from 50 μl up to 200 μl . By contrast, in sensor B, the measurements have been made randomly. In view of the results, plotted in Fig. 11, the differential frequency seems to be less dispersive than the differential notch magnitude. This may be due to tolerances in the fabrication process (embroidery pattern, ground plane fabrication and assembly of the two textile layers), that affects directly the losses of the structure. In any case, the repeatability in the measured range is very acceptable. Using equation (4a), the obtained relative dispersion in all the measurements is less than 11%.

Additionally, the fabricated textile frequency-splitting sensor of Fig. 5 has been applied to drop detection. For this experimental measurement setup, drops of 50 μl (the minimum quantity of DI water that the proposed sensor is able to detect, or sensor resolution) have been deposited in the sensitive region of the sensor. After the textile sensing region absorbs the drop, a split in frequency occurs. The different curves for the transmission coefficient, considering 1 drop, 2 drops and 3 drops are plotted in Fig. 12. Since each drop has the same quantity of liquid (50 μl), it can be expected that the frequency response obtained for each measurement agree with the results of 50 μl , 100 μl and 150 μl shown in Fig. 7, as it occurs to a good approximation. In this set of experiments (considering 3 drops as the dynamic range of the sensor), the measured average sensitivity of the proposed microwave frequency-splitting sensor is found to be $135 \text{ MHz/drop} = 2.7 \text{ MHz}/\mu\text{l}$ (similar to the sensitivity inferred in the measurements of Fig. 8). The data points for the output variables corresponding to the different number of drops are depicted in Fig. 13.

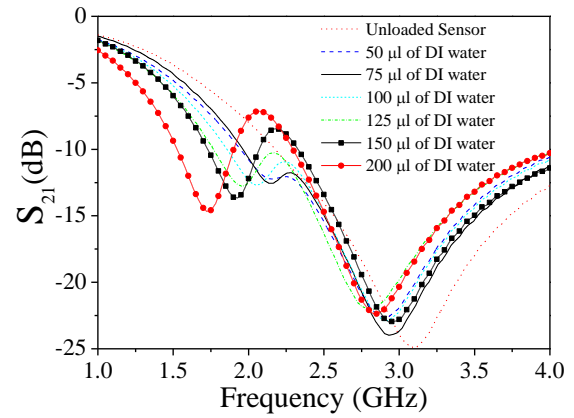


Fig. 7. Measured transmission coefficient (magnitude) for different quantities of absorbed DI water in the sensing region of the proposed sensor.

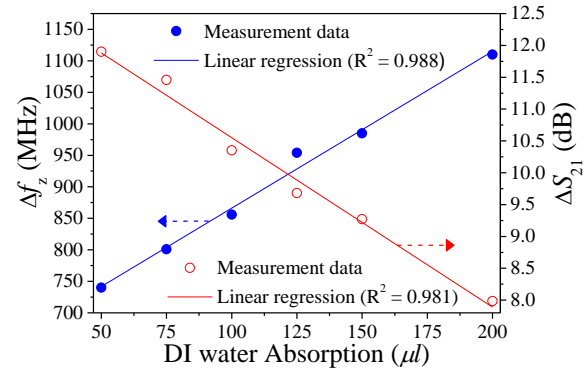


Fig. 8. Representation of measured $\Delta f_z = f_2 - f_1$ and $\Delta S_{21} = S_{21min,2} - S_{21min,1}$ as a function of the amount of absorbed DI water in the sensing region of the fabricated textile differential microwave sensor.

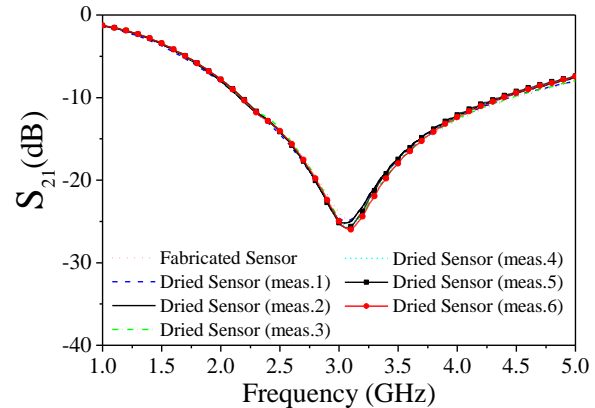


Fig. 9. Measured transmission coefficient (magnitude) of the proposed microwave frequency-splitting sensor after each measurement plotted in Fig. 7 and application of an air dryer.

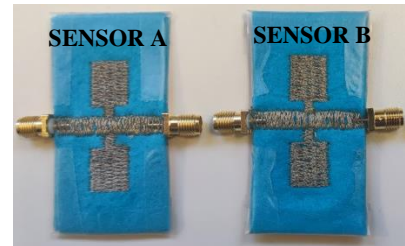


Fig. 10. Fabricated textile frequency-splitting microwave sensors to evaluate the repeatability of the absorption measurements.

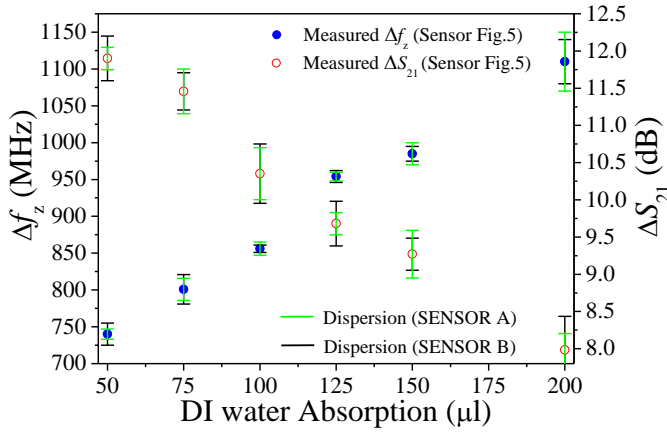


Fig.11. Representation of the dispersion obtained in the measured Δf_z and ΔS_{21} of the sensors in Fig.10 compared to the sensor of Fig.5.

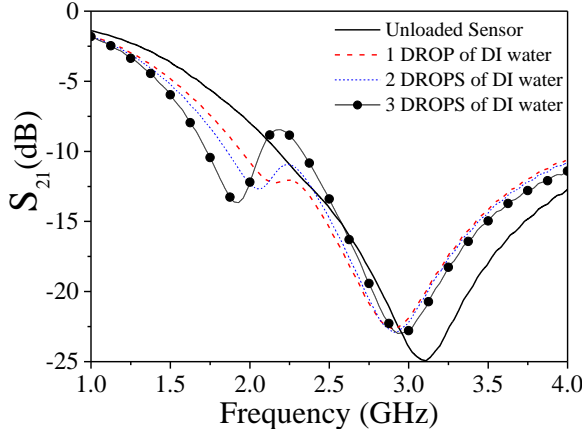


Fig.12. Measured transmission coefficient (magnitude) for different DI water droplets absorbed in the sensing region of the sensor in Fig.5.

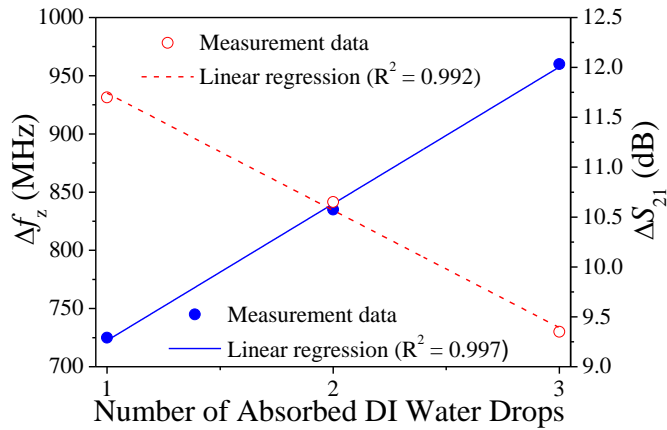


Fig.13. Representation of measured $\Delta f_z = f_2 - f_1$ and $\Delta S_{21} = S_{21min,f2} - S_{21min,f1}$ as a function of the number of absorbed DI water drops in the sensing region of the fabricated textile frequency-splitting microwave sensor.

V. COMPARISON WITH OTHER WEARABLE MICROWAVE SENSORS FOR DIELECTRIC CHARACTERIZATION

Let us now compare the proposed sensor with other textile microwave sensors considering absorption of liquids. It is difficult to find in the available literature other reported sensors based on the same technology (in this case, a full

embroidered textile sensor), working with the same output variable (frequency splitting), and considering the same input variable (absorption of DI water). Thus, in the comparative Table I, the authors have also included works where the sensors are implemented on rigid substrates [23],[30], but the working principle is based on the same approach. The proposed embroidered microwave sensor has shown a good compromise between maximum sensitivity, S_{max} , defined as the variation of the split resonance frequency with the dielectric constant (expressed in MHz), or with the absorbed volume of liquid (expressed in MHz/ μ l), resolution, operating frequency (f_0) and full compatibility with embroidered wearable electronic systems. In [38], a flexible printed microwave sensor is demonstrated to be able to detect DI water with a resolution and sensitivity (in MHz/ μ l) comparable to the one of the presented approach, but such sensor is not based on embroidered techniques. In [39], a circular-ring monopole textile antenna based-sensor for the determination of salinity and sugar concentration through absorption is presented. The reported sensitivity (in MHz/ μ l) and resolution is of the same order, but worse, as compared to the one of the sensor proposed in this paper. Moreover, in [39], a single-ended measurement technique was considered. By contrast, in this work, a quasi-differential technique has been used, and the sensor exhibits robustness against cross-sensitivities caused by environmental factors (as far as they are seen as common-mode stimuli).

In Table I, references [23] and [30] have been included since the operation mode is the same to the one in this work (frequency splitting), as indicated, but such sensors were implemented on rigid (conventional) microwave substrates. The input variable in these sensors is the dielectric constant of the MUT. Thus the sensitivity is expressed in units of MHz. S_{max} in [30] is very high, but such sensor operates at very high frequency. Thus, for a faithful comparison, the relative sensitivity, i.e., $S_{max}/f_0 \equiv S_{max,f_0}$ should be considered (it is included in Table I). In view of the values of S_{max,f_0} , it can be appreciated that the sensor presented in this work is the one exhibiting the highest relative sensitivity. Indeed, in [30], the dielectric material (MUT) was positioned on top of the resonant sensing element (also a SIR), thereby keeping the complex dielectric constant of the substrate (where the sensor is implemented) unaltered. By contrast, in the present work, the liquid modifies the dielectric properties of the textile substrate (where most of the electromagnetic field lines are confined), resulting in an enhancement of the relative sensitivity.

TABLE I
COMPARISON OF VARIOUS MICROWAVE SENSORS FOR DIELECTRIC CHARACTERIZATION

Ref.	f_0 (GHz)	S_{max} (MHz/ μ l)/ S_{max} (MHz)	S_{max,f_0} (%)	Resolution (μ l)	Textile Substrate / Conductive thread
[23]	0.98	- / 3.60	0.36	-	No / No
[30]	60.00	- / 4722	7.87	-	No / No
[39]	2.40	0.80 / -	-	80	Yes / Yes
[38]	2.43	2.20 / -	-	50	No / No
This work	3.00	2.70 / 280	9.3	50	Yes / Yes

VI. CONCLUSIONS

In this work, a frequency-splitting microwave sensor based on stepped-impedance resonators (SIRs) implemented in textile substrate, using an embroider technique, is presented for the first time. The sensor structure is based on a non-woven 100% polyester (PES) textile substrate and conductive thread (*Shieldex 117/17* 2-ply with 99% pure silver-plated nylon yarn 140/17 *dtex*). The sensing principle is based on the asymmetric loading (in one SIR with respect to the other) that the absorption of DI water generates. This affects the effective complex dielectric constant of the textile substrate and therefore produces changes in the frequency response of the transmission coefficient (resonance frequency and magnitude). The proposed textile microwave sensor demonstrates an average sensitivity of 2.51 MHz/ μl and 0.03 dB/ μl in frequency and magnitude, respectively (with a resolution of 50 μl). The presented sensor can also be applied in applications where the detection of small (≈ 50 μl) drops is needed, and the measurements covered the dynamic range between 50-200 μl . It is worth mentioning that in a real scenario, the high-cost vector network analyzer (VNA) can be replaced by a voltage controlled oscillator (VCO) covering the whole frequency span, or output dynamic range (or alternatively a set of VCOs able to cover the desired frequency span of operation). Repeatability in the fabrication process of the proposed sensor has been verified by additional fabrication of two prototypes. The presented textile frequency-splitting microwave sensor exhibits the following advantages: high sensitivity and resolution, good dynamic range, easy fabrication process and wearability. The results derived from this work validate the possibility of implementing textile-based sensors based on frequency splitting, and devoted to absorption measurements. Different topologies, aimed to further enhancing the sensitivity (e.g. by uncoupling the resonant elements), combined with textile substrates, and using embroidery techniques, can be envisaged.

REFERENCES

- [1] A. Ostfeld, I. Deckman, A. Gaikwad, C. Lochner, and A. Arias, "Screen printed passive components for flexible power electronics," *Sci. Rep.*, vol. 15959, no. 5, pp. 1-11, Oct. 2015.
- [2] V. Correia, K.Y. Mitra, H. Castro, J.G. Rocha, E. Sowade, R.R. Baumann, and S. Lanceros-Mendez, "Design and fabrication of multilayer inkjet-printed passive components for printed electronics circuit development," *J. Manuf. Process.*, vol. 31, pp. 364-371, Jan. 2018.
- [3] M. Ali, D. Prakash, T. Zillger, P. K. Singh, and A. C. Hübler, "Printed piezoelectric energy harvesting device", *Adv. Energy Mater.*, vol. 4, no.2, Jan. 2014.
- [4] W. G. Whittow, S. S. Bukhari, L. A. Jones, and I. L. Morrow, "Applications and Future Prospects for Microstrip Antennas using Heterogeneous and Complex 3-D Geometry Substrates," *Prog. Electromagn. Res.*, vol. 144, pp. 271-280, Jan. 2014.
- [5] T. Maleszka, and P. Kabacik, "Bandwidth properties of embroidered loop antenna for wearable applications", *3rd Eur. Wirel. Technol. Conf. (EuWIT)*, Paris, France, Sept. 27-28, 2010.
- [6] T. Acti, A. Chauraya, S. Zhang, W. G. Whittow, R. Seager, J. C. Vardaxoglou, and T. Dias, "Embroidered Wire Dipole Antennas Using Novel Copper Yarns," *IEEE Antennas Wirel. Propag. Lett.*, vol. 14, pp. 638-641, 2015.
- [7] B. Patel, and F. Raval, "Wearable Textile Microstrip Low Pass Filter using Jeans as Substrate," *Int. J. Eng. Res.*, vol.4, no.4, pp. 1438-1441, April 2015.
- [8] B. Moradi, R. Fernández-García, and I. Gil, "Meander Microwave Bandpass Filter on a Flexible Textile Substrate," *Electronics*, vol. 8, no. 11, pp. 1-7, Dec. 2018.
- [9] R. Fernandez-Garcia, and I. Gil, "Textile Yagi antenna at 1.8 GHz," *2017 Prog. Electromagn. Res. Symp. (PIERS)*, St. Petersburg, Russia, May 22-25, 2017.
- [10] H. Xiaomu, S. Yan, and G. A. E. Vandenbosch, "Wearable Button Antenna for Dual-Band WLAN Applications With Combined on and off-Body Radiation Patterns," *IEEE Trans. Antennas and Propag.*, vol. 65, no. 3, pp. 1384-1387, March 2017.
- [11] B. Moradi, M. Martínez, R. Fernández-García, and I. Gil, "Study of Double Ring Resonator Embroidered Wearable Antennas for Microwave Applications," *13th Eur. Conf. Antennas Propag. (EuCAP)*, Krakow, Poland, March 31-5 April, 2019.
- [12] T. Grethe, S. Borczyk, K. Plenkmann, M. Normann, M. Rabe, and A. Schwarz-Pfeiffer, "Textile humidity sensors," *2018 Symp. Des. Test Integr. Packag. MEMS MOEMS DTIP 2018*, Rome, Italy, May 22-25, 2018.
- [13] C. Luo, R. Fernández-García, and I. Gil, "Embroidered Textile Capacitive Sensor for Sucrose Solutions Measurement," *FLEPS 2020 - IEEE Int. Conf. Flex. Printable Sens. Syst. Proc.*, Manchester, UK, Aug. 16-19, 2020.
- [14] D. Elsheikh, and A. R. Eldamak, "Microwave Textile Sensors for Breast Cancer Detection," *2021 38th National Radio Science Conference (NRSC)*, Mansoura, Egypt, July 27-29, 2021.
- [15] M. Martínez-Estrada, I. Gil, and R. Fernández-García, "An Alternative Method to Develop Embroidery Textile Strain Sensors," *Textiles*, vol. 1, no. 3, pp. 504-512, Nov. 2021.
- [16] H. R. Nejad, M. P. Punjiya, and S. Sonkusale, "Washable thread based strain sensor for smart textile," *TRANSDUCERS 2017 - 19th Int. Conf. Solid-State Sens. Actuators Microsyst.*, Kaohsiung, Taiwan, Jun. 18-22, 2017.
- [17] F. J. Ferrández-Pastor, J. M. García-Chamizo, and M. Nieto-Hidalgo, "Electromagnetic differential measuring method: application in microstrip sensors developing," *Sensors*, vol. 17, no. 7, pp. 1-20, July 2017.
- [18] J. Muñoz-Enano, P. Vélez, M. Gil, and F. Martín, "An analytical method to implement high sensitivity transmission line differential sensors for dielectric constant measurements," *IEEE Sensors J.*, vol. 20, no. 1, pp. 178-184, Jan. 2020.
- [19] C. Damm, M. Schüßler, M. Puentes, H. Maune, M. Maasch, and R. Jakoby, "Artificial transmission lines for high sensitive microwave sensors," *2009 IEEE Sensors*, Christchurch, New Zeland, Oct. 25-28, 2010.
- [20] M. A. H. Ansari, A. K. Jha, and M. J. Akhtar, "Design and Application of the CSRR-Based Planar Sensor for Noninvasive Measurement of Complex Permittivity," *IEEE Sensors J.*, vol. 15, no. 12, pp. 7181-7189, Dec. 2015.
- [21] J. Coromina, J. Muñoz-Enano, P. Vélez, A. Ebrahimi, J. Scott, K. Ghorbani, and F. Martín, "Capacitively-loaded slow-wave transmission lines for sensitivity improvement in phase-variation permittivity sensors," *50th European Microwave Conference (EuMC)*, Utrecht, Netherlands, Jan. 12-14, 2021.
- [22] A. Ebrahimi, J. Coromina, J. Muñoz-Enano, P. Vélez, J. Scott, K. Ghorbani, and F. Martín, "Highly sensitive phase-variation dielectric constant sensor based on a capacitively-loaded slow-wave transmission line," *IEEE Trans. Circ. Syst. I: Regular Papers*, vol. 68, no.7, pp. 2787-2799, July 2021.
- [23] P. Vélez, L. Su, K. Grenier, J. Mata-Contreras, D. Dubuc and F. Martín, "Microwave Microfluidic Sensor Based on a Microstrip Splitter/Combiner Configuration and Split Ring Resonators (SRRs) for Dielectric Characterization of Liquids," *IEEE Sensors J.*, vol. 17, no. 20, pp. 6589-6598, Oct. 2017.
- [24] L. Su, J. Muñoz-Enano, P. Vélez, M. Gil-Barba, P. Casacuberta, and F. Martín, "Highly Sensitive Reflective-Mode Phase-Variation Permittivity Sensor Based on a Coplanar Waveguide Terminated With an Open Complementary Split Ring Resonator (OCSRR)," *IEEE Access*, vol. 9, pp. 27928-27944, Feb. 2021.
- [25] J. Muñoz-Enano, P. Vélez, L. Su, M. Gil, P. Casacuberta and F. Martín, "On the Sensitivity of Reflective-Mode Phase-Variation Sensors Based on Open-Ended Stepped-Impedance Transmission Lines: Theoretical Analysis and Experimental Validation," *IEEE Trans. Microw. Theory Techn.*, vol. 69, no. 1, pp. 308-324, Jan. 2021.
- [26] P. Vélez, K. Grenier, J. Mata-Contreras, D. Dubuc and F. Martín, "Highly-Sensitive Microwave Sensors Based on Open Complementary

- Split Ring Resonators (OCSRRs) for Dielectric Characterization and Solute Concentration Measurement in Liquids," *IEEE Access*, vol. 6, pp. 48324-48338, Aug. 2018.
- [27] M. Gil, P. Vélez, F. Aznar-Ballesta, J. Muñoz-Enano, and F. Martín, "Differential Sensor Based on Electroinductive Wave Transmission Lines for Dielectric Constant Measurements and Defect Detection," *IEEE Trans. Antennas Propag.*, vol. 68, no. 3, pp. 1876-1886, March 2020.
- [28] Z. Abbasi, M. Baghelani, and M. Daneshmand, "Disposable Microwave Sensor for Real-time Monitoring and Content Sensing of Droplets in Microfluidic Devices," *2020 IEEE Int. Symp. Antennas Propag. USNC-URSI Radio Sci.*, Montreal, QC, Canada, July 5-10, 2020.
- [29] U. Schwerthoeffer, R. Weigel, and D. Kissinger, "Highly sensitive microwave resonant near-field sensor for precise aqueous glucose detection in microfluidic medical applications," *I2MTC 2014 - 2014 IEEE Int. Instrum. Meas. Technol. Conf.: Discov. New Horiz. Instrum. Meas. Proc.*, Montevideo, Uruguay, May 12-15, 2014.
- [30] J. Naqui, C. Damm, A. Wiens, R. Jakoby, L. Su, and F. Martín, "Transmission lines loaded with pairs of magnetically coupled stepped impedance resonators: Modeling and application to microwave sensors," *IEEE MTT-S Int. Microw. Symp. Dig.*, Tampa, FL, USA, June 1-6, 2014.
- [31] M. Makimoto, and S. Yamashita, "Compact bandpass filters using stepped impedance resonators," *Proc. IEEE*, vol. 67, no. 1, pp. 16-19, Jan. 1979.
- [32] J. Zhong, A. Kiourti, T. Sebastian, Y. Bayram, and J. L. Volakis, "Conformal Load-Bearing Spiral Antenna on Conductive Textile Threads," *IEEE Antennas Wirel. Propag. Lett.*, vol. 16, pp. 230-233, May 2016.
- [33] S. Zhang, A. Chauraya, W. Whittow, R. Seager, T. Acti, T. Dias, and Y. Vardaxoglou, "Embroidered wearable antennas using conductive threads with different stitch spacings," *2012 Loughb. Antennas Propag. Conf. LAPC 2012*, Loughborough, UK, Nov. 12-13, 2012.
- [34] W. Withayachumnankul, K. Jaruwongrunsee, A. Tuantranont, C. Fumeaux, and D. Abbott, "Metamaterial-based microfluidic sensor for dielectric characterization," *Sens. Actuators, A*, vol. 189, no. 15, pp. 233-237, Jan. 2013.
- [35] P. Vélez, K. Grenier, J. Mata-Contreras, D. Dubuc, and F. Martín, "Highly-Sensitive Microwave Sensors Based on Open Complementary Split Ring Resonators (OCSRRs) for Dielectric Characterization and Solute Concentration Measurement in Liquids," *IEEE Access*, vol. 6, pp. 48324-48338, Aug. 2018.
- [36] O. Tangsiriruenart, and G. Stylios, "A novel textile stitch-based strain sensor for wearable end users," *Materials*, vol. 12, no. 9, pp. 1469, May 2019.
- [37] D.M. Pozar, *Microwave Engineering*, 4th Ed., John Wiley, Hoboken, USA, 2012.
- [38] A. Mason, S. Wylie, O. Korostynska, L. E. Cordova-Lopez, and A. I. Al-Shamma'a, "Flexible e-textile Sensors for Real-Time Health Monitoring at Microwave Frequencies," *Int. J. Smart Sens. Intell. Syst.*, vol. 7, no. 1, pp. 1-47, Dec. 2017.
- [39] M. E. Gharbi, M. Martínez-Estrada, R. Fernández-García, and I. Gil, "Determination of Salinity and Sugar Concentration by Means of a Circular-Ring Monopole Textile Antenna-Based Sensor," *IEEE Sensors J.*, vol. 21, no. 21, pp. 23751-23760, Nov. 2021.



Paris Vélez (S'10-M'14-SM'21) was born in Barcelona, Spain, in 1982. He received the degree in Telecommunications Engineering, specializing in electronics, the Electronics Engineering degree, and the Ph.D. degree in Electrical Engineering from the Universitat Autònoma de Barcelona, Spain, in 2008, 2010, and 2014, respectively. His Ph.D. thesis concerned common mode suppression differential microwave circuits based on metamaterial concepts and semi-lumped resonators. During the Ph.D., he was awarded with a pre-doctoral teaching and research fellowship by the Spanish Government from 2011 to 2014. From 2015-2017, he was involved in the subjects related to metamaterials sensors for fluidics detection and characterization at LAAS-CNRS through a TECNIOSpring fellowship cofounded by the Marie Curie program. From 2018 to 2020 he has worked in miniaturization of passive circuits RF/microwave and sensors-based metamaterials through Juan de la Cierva fellowship. His current research interests include the miniaturization of passive circuits RF/microwave and sensors-based metamaterials. Dr. Vélez is a

Reviewer for the IEEE Transactions on Microwave Theory and Techniques and for other journals.



Ferran Martín (M'04-SM'08-F'12) was born in Barakaldo (Vizcaya), Spain in 1965. He received the B.S. Degree in Physics from the Universitat Autònoma de Barcelona (UAB) in 1988 and the PhD degree in 1992. From 1994 up to 2006 he was Associate Professor in Electronics at the Departament d'Enginyeria Electrònica (Universitat Autònoma de Barcelona), and since 2007 he is Full Professor of Electronics. In recent years, he has been involved in different research activities including modelling and simulation of electron devices for high frequency applications, millimeter wave and THz generation systems, and the application of electromagnetic bandgaps to microwave and millimeter wave circuits. He is now very active in the field of metamaterials and their application to the miniaturization and optimization of microwave circuits and antennas. Other topics of interest include microwave sensors and RFID systems, with special emphasis on the development of high data capacity chipless-RFID tags. He is the head of the Microwave Engineering, Metamaterials and Antennas Group (GEMMA Group) at UAB, and director of CIMITEC, a research Center on Metamaterials supported by TECNIO (Generalitat de Catalunya). He has organized several international events related to metamaterials and related topics, including Workshops at the IEEE International Microwave Symposium (years 2005 and 2007) and European Microwave Conference (2009, 2015 and 2017), and the Fifth International Congress on Advanced Electromagnetic Materials in Microwaves and Optics (Metamaterials 2011), where he acted as Chair of the Local Organizing Committee. He has acted as Guest Editor for six Special Issues on metamaterials and sensors in five International Journals. He has authored and co-authored over 650 technical conference, letter, journal papers and book chapters, he is co-author of the book on Metamaterials entitled *Metamaterials with Negative Parameters: Theory, Design and Microwave Applications* (John Wiley & Sons Inc.), author of the book *Artificial Transmission Lines for RF and Microwave Applications* (John Wiley & Sons Inc.), co-editor of the book *Balanced Microwave Filters* (Wiley/IEEE Press) and co-author of the book *Time-Domain Signature Barcodes for Chipless-RFID and Sensing Applications* (Springer). Ferran Martín has generated 21 PhDs, has filed several patents on metamaterials and has headed several Development Contracts.

Prof. Martín is a member of the IEEE Microwave Theory and Techniques Society (IEEE MTT-S). He is reviewer of the IEEE Transactions on Microwave Theory and Techniques and IEEE Microwave and Wireless Components Letters, among many other journals, and he serves as member of the Editorial Board of IET Microwaves, Antennas and Propagation, International Journal of RF and Microwave Computer-Aided Engineering, and Sensors. He is also a member of the Technical Committees of the European Microwave Conference (EuMC) and International Congress on Advanced Electromagnetic Materials in Microwaves and Optics (Metamaterials). Among his distinctions, Ferran Martín has received the 2006 Duran Farell Prize for Technological Research, he holds the Parc de Recerca UAB - Santander Technology Transfer Chair, and he has been the recipient of three ICREA ACADEMIA Awards (calls 2008, 2013 and 2018). He is Fellow of the IEEE and Fellow of the IET.



Raúl Fernández-García received the B.Eng. degree in telecommunications and the M.Eng. degree in electronics from the Universitat Politècnica de Catalunya, Barcelona, in 1997 and 1999, respectively, and the Ph.D. degree from the Universitat Autònoma de Barcelona in 2007. From 1998 to 2001, he worked for Sony, Spain, as a Radiofrequency Engineer, where he developed analog and digital TV tuners. From 2001 to 2007, he was a part-time Assistant Professor of Electronics with the Department of Electronics Engineering, Universitat Autònoma de Barcelona. Funded by the European Marie Curie Program, he worked on devices and circuits reliability at IMEC, Belgium, from 2005 to 2006. From 2008 to 2011, he was a full-time Assistant Professor with the Department of Electronics Engineering, Universitat Politècnica de Catalunya. At present, he is an Associate Professor with the

Department of Electronics Engineering. Dr. Fernandez-Garcia is the author or coauthor of more than 110 papers in international journals and conferences and he has been involved in 18 research projects (six as a Principal Researcher) in different research activities, including reliability, electromagnetic compatibility, and electronic textile. His current scientific interest is focused on wearable sensor development for sport and health applications. He was a recipient of the Best Paper Awards at IPFA 2007.



Ignacio Gil received the degrees in physics and electronics engineering in 2000 and 2003, respectively, and the Ph.D. degree from the Universitat Autònoma de Barcelona, Spain, in 2007. From 2003 to 2008, he was an Assistant Professor of Electronics and a Researcher with the RF-Microwave Group, Electronic Engineering Department, Universitat Autònoma de Barcelona. From 2006 to 2008, he worked for EPSON Europe Electronics GmbH, where he developed high-performance integrated RF CMOS circuits, transceivers, and system design. In 2008, he joined the Electronic Engineering Department, Universitat Politècnica de Catalunya (UPC), Spain, as a Lecturer and a Researcher, where he has been an Associate Professor since 2011. He has been involved in different research activities, including passive and active RF and microwave devices and circuits, metamaterials, EMC, and smart textile electronics. From 2012 to 2014, he worked as the Chairman of the Spanish IEEE EMC Chapter. In 2017, he was an Academic Visitor at the Wireless Communications Research Group, Loughborough University, U.K. Dr. Gil is the coauthor of more than 150 scientific publications and holds 18 patents.